

**NANO EXPRESS**

**Open Access**

# Formation of Ga droplets on patterned GaAs (100) by molecular beam epitaxy

Ming-Yu Li<sup>1</sup>, Yusuke Hirono<sup>2</sup>, Sabina D Koukourinkova<sup>2</sup>, Mao Sui<sup>1</sup>, Sangmin Song<sup>1</sup>, Eun-Soo Kim<sup>1</sup>, Jihoon Lee<sup>1,2\*</sup> and Gregory J Salamo<sup>2</sup>

## Abstract

In this paper, the formation of Ga droplets on photo-lithographically patterned GaAs (100) and the control of the size and density of Ga droplets by droplet epitaxy using molecular beam epitaxy are demonstrated. In extension of our previous result from the journal *Physical Status Solidi A*, volume 209 in 2012, the sharp contrast of the size and density of Ga droplets is clearly observed by high-resolution scanning electron microscope, atomic force microscope, and energy dispersive X-ray spectrometry. Also, additional monolayer (ML) coverage is added to strengthen the result. The density of droplets is an order of magnitude higher on the trench area (etched area), while the size of droplets is much larger on the strip top area (un-etched area). A systematic variation of ML coverage results in an establishment of the control of size and density of Ga droplets. The cross-sectional line profile analysis and root mean square roughness analysis show that the trench area (etched area) is approximately six times rougher. The atomic surface roughness is suggested to be the main cause of the sharp contrast of the size and density of Ga droplets and is discussed in terms of surface diffusion.

## Background

In the last two decades, a number of semiconductor quantum and nanostructures (QNSs) by the strain-driven self-assembly based on Stranski-Krastanow (S-K) growth [1] have been demonstrated in the field of epitaxial growth using molecular beam epitaxy (MBE). As a result, various device applications have been demonstrated such as lasers, detectors, sensors, photovoltaic cells, light-emitting diodes, and solid-state quantum computation [2-7]. Meanwhile, droplet epitaxy (D-E) proposed by Koguchi et al. in 1991 [8] has been relatively recently gaining increased interests due to its advantages over the conventional S-K growth approach for the fabrication of low-dimensional epitaxial semiconductor QNSs [9-23]. While the strain induced by the lattice mismatch is required in the S-K approach, it is not essential in the D-E approach for the fabrication of epitaxial QNSs. As a result, the selection of material system for QNSs by D-E approach is highly elastic and thus, a variety of unseen configurations of epitaxial QNSs have

been demonstrated by D-E approach [9-23]. In addition, not only D-E approach can be used for lattice matched systems but also can be applied in the lattice mismatched systems. Quantum dots (QDs) and quantum rings are the most commonly studied epitaxial QNSs [9-14]. QD molecules [15-19], low-density QDs [20], ensembles of quantum ring geometry and droplet [21], and various nanostructure complexes [22,23] have been demonstrated by the D-E approach. In addition, nano-hole drilling and local etching effect [24-26], selective etching using droplet as a mask [27,28], various configurations of In nanocrystals [29,30], running droplets [31-33], and Ga-triggered oxide desorption [34,35] are only a few examples of D-E applications.

The fabrication of epitaxial QNSs is inherently dependent on the size, shape, and density of initial liquid phase metal droplets (MDs) and consequently, the control of the density and size of MDs becomes an essential research focus. The control of droplets on planar substrates has been somewhat widely studied [9-23,36,37]; however, the fabrication of MDs on patterned surfaces lacks its investigation. This very naturally puts the control of MDs on patterned substrate as an attractive and essential research topic. In this paper, therefore, in

\* Correspondence: jihoonlee@kw.ac.kr

<sup>1</sup>College of Electronics and Information, Kwangwoon University, Nowon-gu Seoul 139-701, South Korea

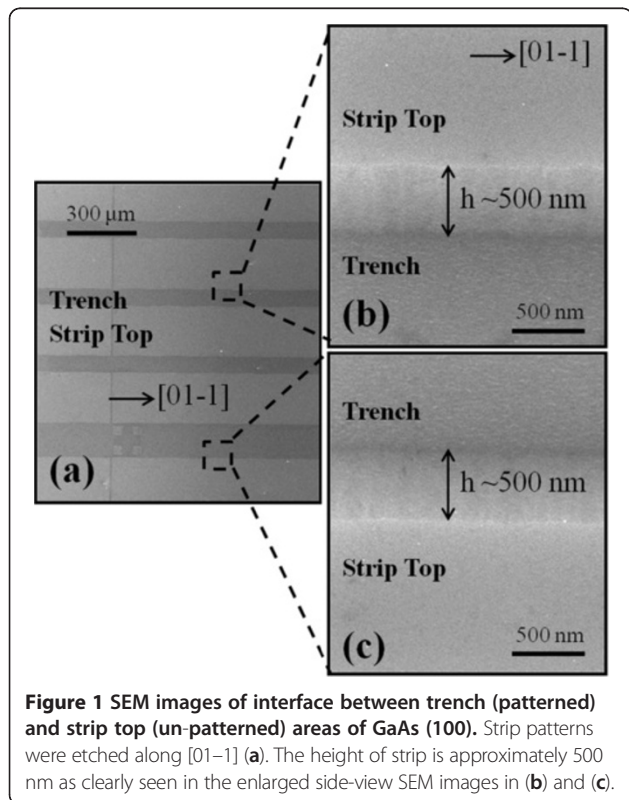
<sup>2</sup>Institute of Nanoscale Science and Engineering, University of Arkansas, Fayetteville 72701, AR, USA

extension of our previous results [38,39], we extend the results of the sharp contrast of the size and density of Ga MDs on photo-lithographically patterned GaAs (100) by D-E approach using MBE. As evidenced by 3-D atomic force microscope (AFM) and high-resolution scanning electron microscope (SEM), the sharp contrast of the size and density of Ga MDs is clearly observed, showing an order magnitude higher density on the trench area (the etched area). Conversely, the size is much larger on strip top area (the un-etched area). By systematically varying the monolayer (ML) coverage, we demonstrate the control of size and density of Ga MDs on patterned GaAs (100) surface. The atomic surface roughness is around six times higher on the trench area (etched area) based on the cross-sectional line profile and root mean square (RMS) roughness analysis. The sharp contrast of size and density of Ga MDs is discussed in terms of surface adatom diffusion.

## Methods

### Experimental details

The strip patterns used in this experiment were fabricated using conventional photolithography technique and wet chemical etching. As clearly shown in Figure 1 (a), the strip patterns were fabricated on GaAs (100) along [01-1] and the width of strips are approximately 220  $\mu\text{m}$  and of the trenches are approximately 70  $\mu\text{m}$ .



The height of the strip pattern is approximately 500 nm as clearly seen in Figure 1 (b, c), which are cutouts from the Figure 1 (a). The 'strip top' area was covered by photo-resist during the etching using a  $\text{H}_3\text{PO}_4\text{:H}_2\text{O}_2\text{:H}_2\text{O}$  (3:1:100) solution while the 'trench' area was exposed. For the fabrication of Ga MDs on strip-patterned GaAs (100) surfaces, a Riber-32P solid-source MBE was used. To observe the substrate temperature ( $T_{\text{sub}}$ ) and growth rate ( $G_{\text{rate}}$ ) of surface reconstructions and growth procedures, an *in-situ* reflection high-energy electron diffraction was utilized. For a consistent set of experiments, growth procedures were kept similarly between samples. After mounting the samples on molybdenum sample holder block (moly-block), it was degassed at the  $T_{\text{sub}}$  of 350°C for an hour. Then the moly-block was introduced in a main growth chamber through ultra-high vacuum transfer modules. The  $T_{\text{sub}}$  was then raised to 600°C by 50°C/min. Subsequently, by annealing substrates at the  $T_{\text{sub}}$  of 600°C for 10 min the native Ga surface oxide ( $\text{Ga}_2\text{O}_3$ ) was removed. From our previous experiments on buffer growth on shallow patterned substrates, the buffer growth destroyed the pattern shapes (trenches were filled and sidewalls were smoothed) due to high anisotropic surface diffusion during the buffer growth [40,41]. Thus, a buffer layer was avoided in this experiment. After annealing the  $T_{\text{sub}}$  was lowered to 400°C for the fabrication of Ga MDs. For the consistency of the results and minimization of the arsenic monomer background, the chamber background pressure was kept below  $4 \times 10^{-9}$  Torr for each growth. The arsenic monomer background pressure was below  $10^{-12}$  Torr under this pressure. Now based on an equivalent amount of GaAs growth with  $\text{As}_4$  flux, 20, 10, and 5 ML of Ga were deposited on strip-patterned GaAs (100) surfaces at the  $T_{\text{sub}}$  at 400°C to form metal Ga droplets. The  $G_{\text{rate}}$  used was 0.5 ML/s. Then, the  $T_{\text{sub}}$  was quenched down right after the fabrication in order to minimize Ostwald ripening [42,43]. An SEM under vacuum and AFM in air was used for the characterization of surface morphology [44-46]. Energy dispersive X-ray spectrometry (EDS) under vacuum was used for the chemical composition analysis and NanoScope (Bruker Corporation, Billerica, MA, USA), WSXM Nanotec Electronica S.L, Tres Cantos (Madrid) SPAIN [47] and Origin software (Origin Software Inc., San Clemente, CA, USA) were used for the analysis and processing of the acquired data.

## Results and discussion

Figure 2 shows the sharp contrast of the density and size of Ga MDs at the interface between trench and strip top areas by the SEM images. The Ga MDs were fabricated with 20 ML at the surface temperature ( $T_{\text{sub}}$ ) of 400°C. Figure 2 (b) is a cutout from the Figure 2 (a) and

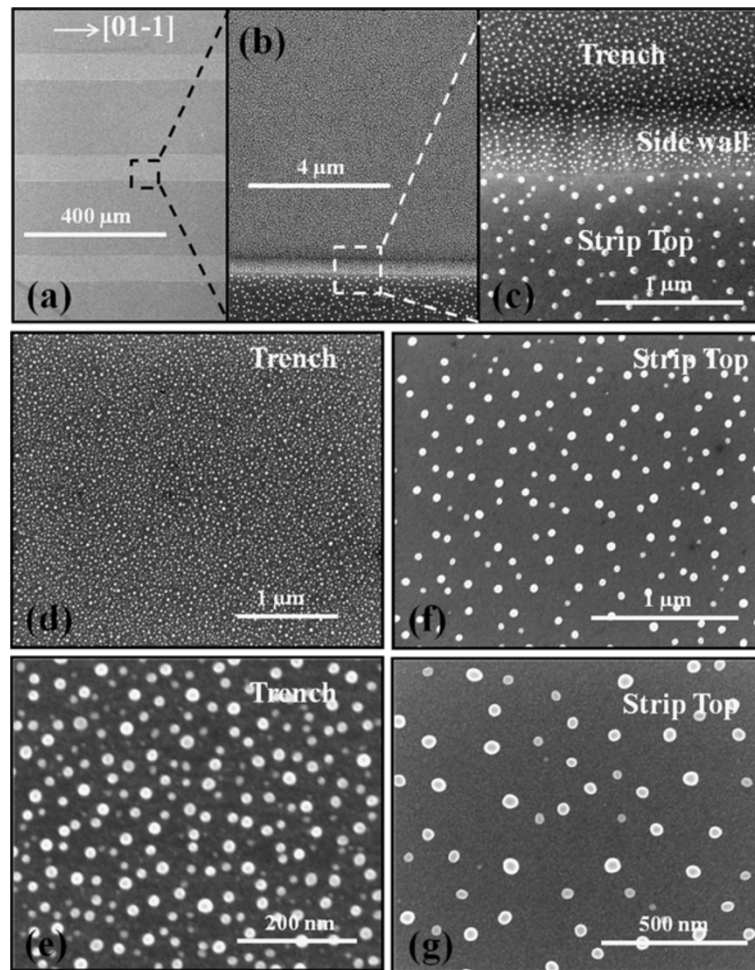


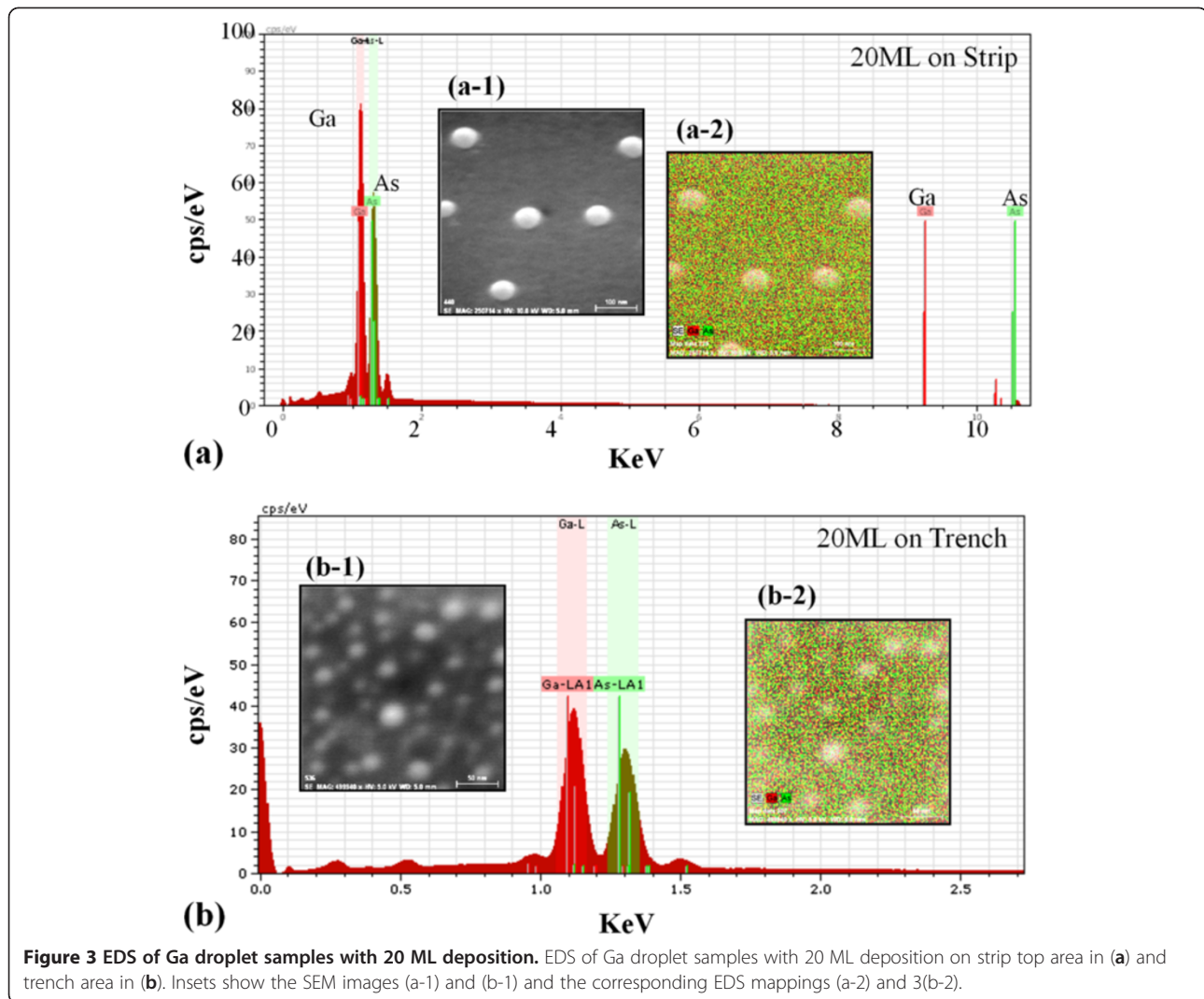
**Figure 2** SEM images of the interface between trench (patterned) and strip top (un-patterned) areas of GaAs (100). SEM images of the interface between the trench (patterned) and strip top (un-patterned) areas of GaAs (100) showing the sharp contrast of size and density of Ga metal droplets. Ga droplets were fabricated with the deposition of 20 ML at the  $T_{\text{sub}}$  of 400°C.

similarly, Figure 2 (c) is from Figure 2 (b). With an enlarged view of Figure 2 (c) at the interface between etched and un-etched areas, the sharp contrast in size and density is clearly observed between the strip top and trench areas. In Figure 2, (d) and (f) are further enlarged images of trench areas and in the same way in Figure 2, (e) and (g) are from strip top areas. By comparing the strip top and trench areas, the density of Ga MDs is relatively higher and the size is much smaller on the trench area. Meanwhile, the density of MDs is much lower and the size is much larger on the strip top area. As the image size of Figure 2 (f) is almost twice as large as Figure 2 (g), the size of MDs on strip top area in Figure 2 (g) is indeed much larger. Figure 3 shows EDS analysis of Ga MD samples with 20 ML deposition on both strip top area in Figure 3a and trench area in Figure 3b. The EDS analysis confirmed the presence of elemental signal of Ga and As and the higher Ga peaks

as expected. The SEM insets and EDS mappings show good matching and the MDs are indeed consisted of Ga as clearly shown in Figure 3 (a-2) and (b-2).

A systematic variation of Ga ML deposition on strip-patterned GaAs (100) is demonstrated and shown in Figures 4 and 5; the summary plots of density, diameter, and height are shown in Figure 6. Figure 4 shows 2-D flat AFM views of Ga MD formation on the strip and trench areas with 20 ML in Figure 4a,b and with 10 ML in Figure 4c,d and 5 ML in Figure 4e,f. For the side-view perspective, Figure 5 shows the 3-D side AFM views of Ga MDs similarly with 20, 10, and 5 ML. With 5-ML deposition, the average density was  $2.8 \times 10^9 \text{ cm}^{-2}$  on trench area, while it was  $3.8 \times 10^8 \text{ cm}^{-2}$  on the strip area. There was about an order of magnitude difference between the strip and trench areas. With an increase of ML to 10, the density was increased to  $4.2 \times 10^{10} \text{ cm}^{-2}$  on the trench and to  $4.9 \times 10^9 \text{ cm}^{-2}$  on strip. Also, there





was about an order of difference between the two areas in the average density of Ga MDs. With a further increase of ML deposition to 20, the average density was slightly decreased to  $3.68 \times 10^{10} \text{ cm}^{-2}$  on the trench area and to  $3.9 \times 10^9 \text{ cm}^{-2}$  on strip area. In previous experiments, an increase of the average MD density was observed when ML deposition was increased [36,37]. Also, slightly reduced density was observed depending on the growth conditions, i.e., duration,  $G_{\text{rate}}$ , and  $T_{\text{sub}}$ . Here the  $T_{\text{sub}}$  was fixed at  $400^\circ\text{C}$  and the  $G_{\text{rate}}$  was also fixed at  $0.5 \text{ ML/s}$  for all samples. Thus, the growth duration was increased with increased deposition amount. With 5-ML deposition, the MDs began to nucleate, and the density and size were increased when ML deposition was increased to 10, reaching the peak density. With a further increase of ML to 20, which is equivalent to the duration of 40 s in this experiment, the MDs could have sufficient time to diffuse

and merge. Once the merging of MDs occurs, bigger MDs tend to absorb the smaller ones and this process can result in a reduced density, which is known as Ostwald-ripening [42,43]. To minimize Ostwald-ripening, the duration has to be reduced but this requires a variation of the growth parameter,  $G_{\text{rate}}$  in this case. For the diameters of MDs, the average diameters were larger on strip top areas as clearly seen in Figure 6b as well as in the AFM images of Figures 4 and 5. Both the strip and trench pattern show increased average diameters when ML was increased. At 5 ML on strip, the diameter was 40 nm and increased to 63 nm with 10 ML and to 105 nm with 20 ML. On the trench areas, the average diameters of Ga MDs were 38.2 nm with 5 ML, 60 nm with 10 ML, and 86 nm with 20 ML. As the ML deposition was increased, the gap between the strip top and trench areas became larger perhaps due to Ostwald-ripening as discussed. The increased

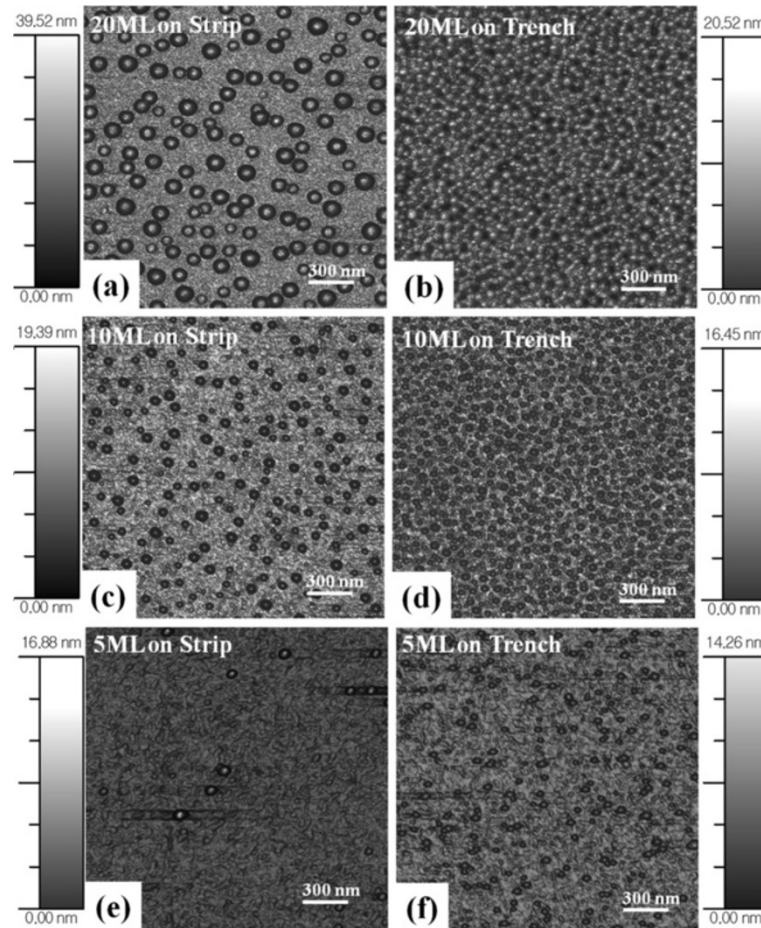


**Figure 4 3-D top-view atomic force microscope (AFM) images.** 3-D top-view atomic force microscope (AFM) images show the surface morphologies of Ga metal droplets on GaAs (100) with 20, 10, and 5-ML depositions at the  $T_{\text{sub}}$  of 400°C. AFM images are  $2(x) \times 2(y) \mu\text{m}^2$ , and scale bars correspond to the heights of the images.

diameter of Ga MDs is a common trend with increase in deposition amount [36,37]. Now, for the average height of Ga MDs as seen in Figure 6c, on strip top areas, it showed a constant increase. An increased height of MDs is also an acceptable result when ML deposition is increased in conditions of atomically smooth surfaces. However, the height of MDs on trench areas kept almost the same regardless of the ML variation in this experiment. This indicates that the amount of deposition was dedicated either to the expansion of diameter or to the increase of density if there was no intermixing or desorption involved in the process [36,37]. Considering the  $T_{\text{sub}}$  of MD fabrication, we could exclude the intermixing and desorption to some degree. The diameter of Ga MDs in Figure 6b does not seem to be unusual, indicating the blue line stays below the black. The density of MDs on the trench area (blue line in Figure 6a) shows that the increased deposition was mostly used for the increase of density; the

blue line stays above black. Also, this behavior can indicate that the surface is not atomically smooth on the trench area.

Figure 7 shows the cross-sectional line profiles (CLPs) of bare GaAs (100) on strip area in Figure 7a and trench area in Figure 7b before Ga MD fabrication. Figure 7c is the CLP on the strip area and likewise, Figure 7d is on trench area shown as white lines in Figure 7a, b. The lengths of CLPs are  $5 \mu\text{m}$  ( $x$ -axes on the graphs), and height was set at 10 nm for a straightforward comparison. As clearly seen in CLPs, the trench area is much rougher, confirming the previous speculation based on MD size analyses. The strip area showed an RMS roughness of 0.39, while the trench area was 2.26 which indicates that the trench area is approximately 5.8 times rougher. This large difference on the atomic surface roughness could be the major cause for the sharp contrast on the size and density of Ga MDs. A smoother surface can indicate a longer diffusion length and *vice*

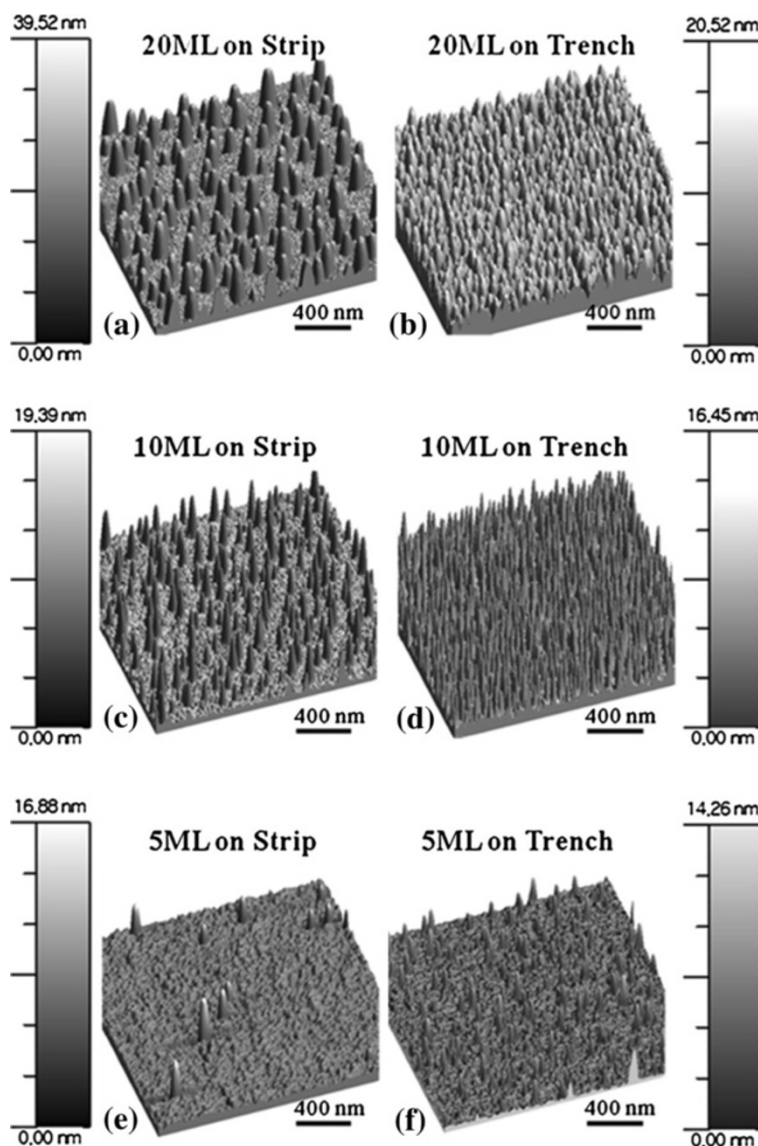


**Figure 5** 3-D side-view AFM images of the variation of Ga metal droplets; 20 in (a) and (b), 10 in (c) and (d), and 5-ML depositions in (e) and (f) at the  $T_{\text{sub}}$  of 400°C. Figures correspond to the images in Figure 4: Figures 4a-5a, etc.

*versa*. When the diffusion length is longer, we generally observe lower density and larger size of MDs, for example, Ga and In MDs [36,37]. We can easily observe the effect of diffusion length when  $T_{\text{sub}}$  is increased and when other conditions were kept the same, as a higher  $T_{\text{sub}}$  indicates a longer diffusion length. For example, the MDs which are fabricated at 500°C as compared to 400°C should have larger dimensions and thus lower density and *vice versa*. In this experiment, the density is nearly an order of magnitude higher on strip areas almost constantly for 5, 10, and 20 ML. Also, the average diameters are larger on strip patterns as the surface is much smoother.

## Conclusions

In conclusion, the sharp contrast of the size and density of Ga MDs on photo-lithographically patterned GaAs (100) was demonstrated and clearly observed by SEM and AFM. The EDS analysis confirmed that the MDs were consisted of Ga atoms. Also a systematic control of size and density was demonstrated by ML variation, and the behavior was discussed with atomic surface roughness, diffusion length, and surface diffusion. Ga MDs were fabricated by solid-source MBE, and the density of MDs was generally higher on the trench areas, and the size was larger on strip tops due to the approximately  $5.8 \times$  smoother surface morphology.

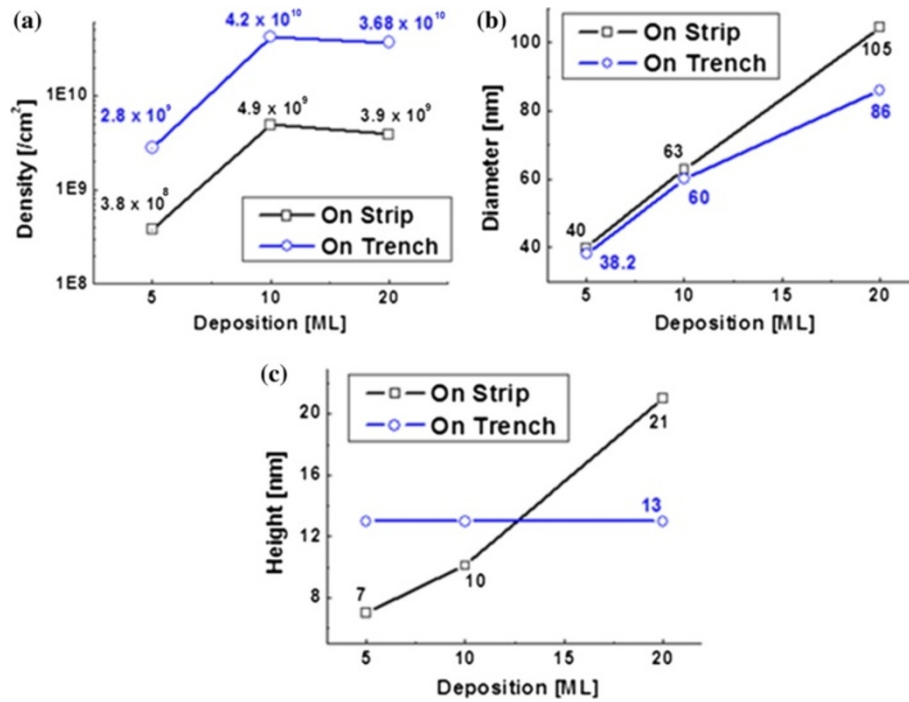


**Figure 6** Plots of density, diameter and height of Ga metal droplets with variation of ML deposition. Data from the strip top and trench are plotted together per each deposition for a straightforward comparison.

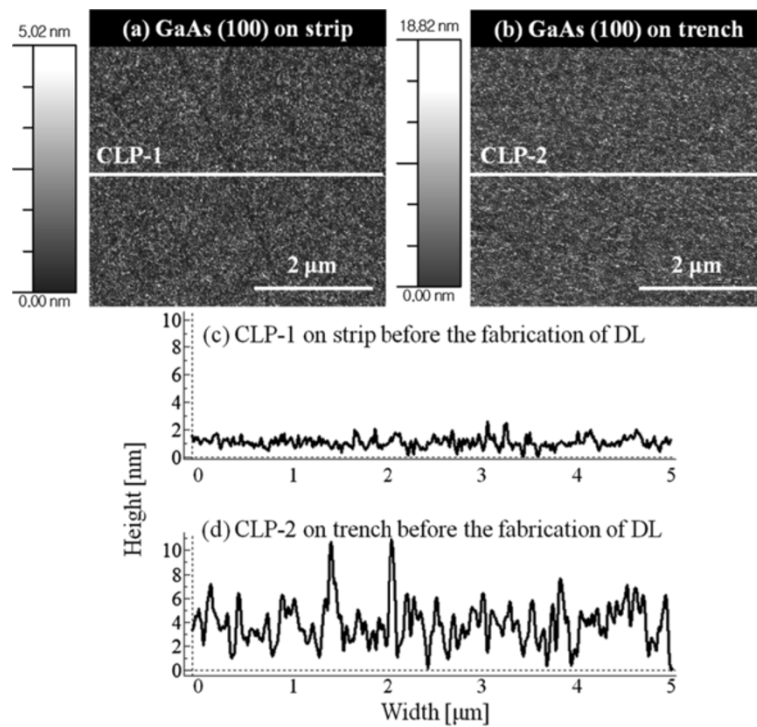


**Figure 7** AFM images of GaAs (100) on strip top and trench area before fabrication of Ga MDs. AFM images of GaAs (100) on (a) strip top area and (b) trench area before the fabrication of Ga MDs. (c) and (d) show the cross-sectional line profiles (CLPs) of two areas. White lines in (a) and (b) are the corresponding locations of CLPs shown in (c) and (d).



### Competing interests

The authors declare that they have no competing interests.

### Authors' contributions

JL, YH, SK participated in the experiment design and carried out the experiments. ML, MS, SS, EK, JL participated in the analysis of data. GS, JL designed the experiments and testing methods. ML, JL carried out writing. All authors helped in drafting and read and approved the final manuscript.

### Acknowledgements

The authors acknowledge the financial support of the NSF through grant number DMR-0520550 and the National Research Foundation of Korea funded by the Ministry of Education, Science and Technology (Grant number 2010-0008394 and 2011-0030821).

Received: 9 July 2012 Accepted: 17 September 2012

Published: 3 October 2012

### References

1. Stranski IN, Krastanov L: **Theory of orientation separation of ionic crystals.** *Sitzber Akad Wiss Wien, Math-naturw Klasse Abt IIb* 1938, **146**:797–810.
2. Cataluna MA, Viktorov EA, Mandel P, Sibbett W, Livshits DA, Weimert J, Kovsh AR, Rafailov EU: **Temperature dependence of pulse duration in a mode-locked quantum-dot laser.** *Appl Phys Lett* 2007, **90**:101102.
3. Lim H, Tsao S, Zhang W, Razeghi M: **High-performance InAs quantum-dot infrared photodetectors grown on InP substrate operating at room temperature.** *Appl Phys Lett* 2007, **90**:131112.
4. Monat, Alloing B, Zinoni C, Li LH, Fiore A: **Nanostructured current-confined single quantum dot light-emitting diode at 1300 nm.** *Nano Lett* 2006, **6**:1464.
5. Wei G, Forrest SR: **Intermediate-band solar cells employing quantum dots embedded in an energy fence barrier.** *Nano Lett* 2007, **7**:218.
6. Duijjs EF, Findeis F, Deutschmann RA, Bichler M, Zrenner A, Abstreiter G, Adlkofer K, Tanaka M, Sackmann E: **Influence of thiol coupling on photoluminescence of near surface InAs quantum dots.** *Phys Stat Sol (B)* 2001, **224**:871.
7. Stinaff EA, Scheibner M, Bracker AS, Ponomarev IV, Korenev VL, Ware ME, Doty MF, Reinecke TL, Gammon D: **Optical signatures of coupled quantum dots.** *Science* 2006, **311**:636.
8. Koguchi N, Takahashi S, Chikyow T: **New MBE growth method for InSb quantum well boxes.** *J Cryst Growth* 1991, **111**:688–692.
9. Mano T, Abbarchi M, Kuroda T, Mastrandrea CA, Vinattieri A, Sanguinetti S, Sakoda K, Gurioni M: **Ultra-narrow emission from single GaAs self-assembled quantum dots grown by droplet epitaxy.** *Nanotechnology* 2009, **20**:395601.
10. Lee JH, Wang ZM, Salamo GJ: **The control on size and density of InAs QDs by droplet epitaxy.** *IEEE T-NANO* 2009, **8**:431.
11. Mano T, Kuroda T, Sanguinetti S, Ochiai T, Tateno T, Kim J, Noda T, Kawabe M, Sakoda K, Kido G, Koguchi N: **Self-assembly of concentric quantum double rings.** *Nano Lett* 2005, **5**:425.
12. Pankaow N, Panyakeow S, Ratanathamaphan SJ: **Formation of  $\text{In}_{0.5}\text{Ga}_{0.5}\text{As}$  ring-and-hole structure by droplet molecular beam epitaxy.** *J Cryst Growth* 2009, **311**:1832.
13. Lee JH, Wang ZM, Ziad YA, Strom NW, Salamo GJ: **Design of nanostructure complexes by droplet epitaxy.** *Cryst Growth Des* 2009, **9**:715.
14. Li S-S, Long G-L, Baii F-S, Feng S-L, Zheng H-Z: **Quantum computing.** *Proc Nat Acad Sci* 2001, **98**:11847.
15. Lee JH, Wang Zh M, Strom NW, Mazur Yu I, Salamo GJ: **InGaAs quantum dot molecules around self-assembled GaAs nanomound templates.** *Appl Phys Lett* 2006, **89**:202101.
16. Lee JH, Sablon K, Wang ZM, Salamo GJ: **Evolution of InGaAs quantum dot molecules.** *J Appl Phys* 2008, **103**:054301.
17. Hanke M, Wang ZM, Lee JH, Salamo GJ, Schmidbauer M: **Step bunch assisted two dimensional ordering of  $\text{In}_{0.19}\text{Ga}_{0.81}\text{As}$ /GaAs quantum dots on vicinal GaAs(001) surfaces.** *Appl Phys Lett* 2008, **92**:033111.
18. Dubslaff AM, Hanke M, Burghammer M, Schoder S, Hoppe R, Schroer CG, Mazur Yi, Wang ZM, Lee JH, Salamo GJ: **InGaAs/GaAs(001) quantum dot molecules probed by nanofocus high resolution X-ray diffraction with 100 nm resolution.** *Appl Phys Lett* 2011, **98**:213105.
19. Creasey M, Li X, Lee JH, Wang ZM, Salamo GJ: **Strongly confined excitons in self-assembled InGaAs quantum dot clusters produced by a hybrid growth method.** *J Appl Phys* 2010, **107**:104302.
20. Liang BL, Wang ZM, Lee JH, Sablon K, Mazur Yi, Salamo GJ: **Low density InAs quantum dots grown on GaAs nanoholes.** *Appl Phys Lett* 2006, **89**:043113.
21. Lee JH, Wang ZM, Sablon K, Salamo GJ: **Formation of hybrid molecules composed of Ga metal particle in direct contact with InGaAs semiconductor quantum ring.** *Cryst Growth Des* 2008, **8**:690.
22. Maruyama T, Otsubo H, Kondo T, Yamamoto Y, Naritsuk S: **Fabrication of GaN dot structure by droplet epitaxy using  $\text{NH}_3$ .** *J Cryst Growth* 2007, **301–302**:486–489.
23. Lee JH, Wang Zh M, AbuWaar ZY, Salamo GJ: **Design of nanostructure complexes by droplet epitaxy.** *Cryst Growth Des* 2009, **9**:715.
24. Wang ZM, Liang BL, Sablon KA, Salamo GJ: **Nanoholes fabricated by self-assembled gallium nanodroplet on GaAs(100).** *Appl Phys Lett* 2007, **90**:113120.
25. Wang ZM, Holmes K, Shultz JL, Salamo GJ: **Self-assembly of GaAs holed nanostructures by droplet epitaxy.** *Phys Stat Sol (A)* 2005, **202**:R85.
26. Stemmann A, Heyn C, Köppen T, Kipp T, Hansen W: **Local droplet etching of nanoholes and rings on GaAs and AlGaAs surfaces.** *Appl Phys Lett* 2008, **93**:123108.
27. Lee JH, Wang ZM, Hirono YK, Dorogan VG, Mazur Yi, Kim ES, Koo SM, Park SH, Song SM, Salamo GJ: **Low-density quantum dot molecules by selective etching using In droplet as a mask.** *IEEE T-NANO* 2011, **10**:600.
28. Lee JH, Wang ZM, Hirono YK, Kim ES, Koo SM, Dorogan VG, Mazur Yi, Song SM, Park GY, Salamo GJ: **InGaAs quantum dot molecules during selective etching using In droplet mask.** *J Phys D: Appl Phys* 2011, **44**:025102.
29. Lee JH, Wang ZM, Hirono YK, Kim ES, Kim NY, Park SH, Wang C, Salamo GJ: **Various configurations of In nanostructures on GaAs (100) by droplet epitaxy.** *CrystEngComm* 2010, **12**:3404.
30. Lee JH: **Instability of various configurations of in nano-crystals on GaAs (100) by droplet epitaxy.** *CrystEngComm* 2011, **13**:771.
31. Tersoff J, Jesson DE, Tang WX: **Running droplets of gallium from evaporation of gallium arsenide.** *Science* 2009, **324**:236–238.
32. Hilner E, Zakharov AA, Schulte K, Kratzer P, Andersen JN, Lundgren E, Mikkelsen A: **Ordering of the nanoscale step morphology as a mechanism for droplet self-propulsion.** *Nano Lett* 2009, **9**:2710–2714.
33. Jiang W, Wang ZM, Li AZ, Benamara M, Li S, Salamo GJ: **Nanoscale footprints of self-running gallium droplets on GaAs surface.** *PLoS One* 2011, **6**:e20765.
34. Lee JH, Wang ZM, Salamo GJ: **Ga-triggered oxide desorption from GaAs (100) and non-(100) substrates.** *Appl Phys Lett* 2006, **88**:252108.
35. Lee JH, Wang ZM, Salamo GJ: **Survival of atomic monolayer steps during oxide desorption on GaAs (100).** *J Appl Phys* 2006, **100**:114330.
36. AbuWaar ZY, Wang ZM, Lee JH, Salamo GJ: **Observation of Ga droplet formation on (311)A and (511)A GaAs surfaces.** *Nanotechnology* 2006, **17**:4037.
37. Lee JH, Wang ZM, Salamo GJ: **Observation of change in critical thickness of In droplet formation on GaAs(100).** *J Phys: Condens Matter* 2007, **19**:176223.
38. Li MY, Lee JH, Wang ZM, Hirono YK, Wu J, Song SM, Koo SM, Kim ES, Salamo GJ: **Sharp contrast of the density and size of Ga metal droplets on photolithographically patterned GaAs (100) by droplet epitaxy under an identical growth environment.** *Phys Status Solidi A* 2012, **209**(6):1075–1079.
39. Gao L, Hirono YK, Li MY, Wu J, Song SM, Koo SM, Kim ES, Wang ZM, Lee JH, Salamo GJ: **Observation of Ga metal droplet formation on photolithographically patterned GaAs (100) surface by droplet epitaxy.** *IEEE T-NANO* 2012, **11**:985.
40. Wang ZM, Lee JH, Liang BL, Black WT, Kunets VP, Mazur Yi, Salamo GJ: **Localized formation of InAs quantum dots on shallow-patterned GaAs (100).** *Appl Phys Lett* 2006, **88**:233102.
41. Lee JH, Wang ZM, Black WT, Kunets VP, Mazur Yi, Salamo GJ: **Spatially localized formation of InAs quantum dots on shallow patterns regardless of crystallographic directions.** *Adv Funct Mater* 2007, **17**:3187.
42. Yao JH, Elder KR, Guo H, Grant M: **Theory and simulation of Ostwald ripening.** *Phys Rev B* 1993, **47**:14110–14125.
43. Glasner K, Otto F, Rump T, Slepcev D: **Ostwald ripening of droplets: the role of migration.** *Eur J Appl Math* 2009, **20**:1–67.
44. Pandey N, Henny B: **Effect of additive noise on phase measurement in digital holographic microscopy.** *3D Research* 2011, **02**:01006.



45. Mann CJ, Bingham PR, Lin HK, Paquit VC, Gleason SS: **Dual modality live cell imaging with multiple-wavelength digital holography and epi-fluorescence.** *3D Research* 2011, **02**:01005.
46. Merola F, Miccio L, Coppola S, Vespini V, Paturzo M, Grilli S, Ferraro P: **Exploring the capabilities of digital holography as tool for testing optical microstructures.** *3D Research* 2011, **02**:01003.
47. Horcas I, Fernandez R, Gomez-Rodriguez JM, Colchero J, Gomez-Herrero J, Baro AM: **WSXM: a software for scanning probe microscopy and a tool for nanotechnology.** *Rev Sci Instrum* 2007, **78**:013705.

doi:10.1186/1556-276X-7-550

**Cite this article as:** Li et al.: Formation of Ga droplets on patterned GaAs (100) by molecular beam epitaxy. *Nanoscale Research Letters* 2012 7:550.

**Submit your manuscript to a SpringerOpen<sup>®</sup> journal and benefit from:**

- ▶ Convenient online submission
- ▶ Rigorous peer review
- ▶ Immediate publication on acceptance
- ▶ Open access: articles freely available online
- ▶ High visibility within the field
- ▶ Retaining the copyright to your article

---

Submit your next manuscript at ▶ [springeropen.com](http://springeropen.com)

---